Anomalously temperature-dependent thermal conductivity of monolayer GaN with large deviations from the traditional 1/T law

Guangzhao Qin,[1] Zhenzhen Qin,[2] Huimin Wang,[1] and Ming Hu[1,3,*]

[1] *Institute of Mineral Engineering, Division of Materials Science and Engineering, Faculty of Georesources and Materials Engineering, RWTH Aachen University, Aachen 52064, Germany*

[2] *College of Electronic Information and Optical Engineering, Nankai University, Tianjin 300071, China*

[3] *Aachen Institute for Advanced Study in Computational Engineering Science (AICES), RWTH Aachen University, Aachen 52062, Germany*

(Received 23 December 2016; revised manuscript received 8 March 2017; published 15 May 2017)

Efficient heat dissipation, which is featured by high thermal conductivity, is one of the crucial issues for the reliability and stability of nanodevices. However, due to the generally fast $1/T$ decrease of thermal conductivity with temperature increase, the efficiency of heat dissipation quickly drops down at an elevated temperature caused by the increase of work load in electronic devices. To this end, pursuing semiconductor materials that possess large thermal conductivity at high temperature, i.e., slower decrease of thermal conductivity with temperature increase than the traditional $\kappa \sim 1/T$ relation, is extremely important to the development of disruptive nanoelectronics. Recently, monolayer gallium nitride (GaN) with a planar honeycomb structure emerges as a promising new two-dimensional material with great potential for applications in nano- and optoelectronics. Here, we report that, despite the commonly established $1/T$ relation of thermal conductivity in plenty of materials, monolayer GaN exhibits anomalous behavior that the thermal conductivity almost decreases linearly over a wide temperature range above 300 K, deviating largely from the traditional $\kappa \sim 1/T$ law. The thermal conductivity at high temperature is much larger than the expected thermal conductivity that follows the general $\kappa \sim 1/T$ trend, which would be beneficial for applications of monolayer GaN in nano- and optoelectronics in terms of efficient heat dissipation. We perform detailed analysis on the mechanisms underlying the anomalously temperature-dependent thermal conductivity of monolayer GaN in the framework of Boltzmann transport theory and further get insight from the view of electronic structure. Beyond that, we also propose two required conditions for materials that would exhibit similar anomalous temperature dependence of thermal conductivity: large difference in atom mass (huge phonon band gap) and electronegativity (LO-TO splitting due to strong polarization of bond). Our study offers fundamental understanding of phonon transport in monolayer GaN, and the insight gained from this study is of great significance for the design and search of materials superior for applications in nano- and optoelectronics in terms of high-performance thermal management.

DOI: 10.1103/PhysRevB.95.195416

I. INTRODUCTION

Two-dimensional (2D) materials with graphene as a representative have been intensively studied for many years for their promising applications in nanoelectronics, which is one of the leading topics in condensed matter physics and materials science [1–5]. Efficient heat dissipation is a crucial issue for the reliable performance and stable function of nanodevices based on these 2D materials, such as field-effect transistor and light-emitting diode (LEDs), especially for the high-power situations where large operating current densities trigger more joule heating [6]. High thermal conductivity is an important indicator for the high-performance thermal management. Due to the fact that the operating temperature is variational when device is switched on, for example, the temperature usually rises up with the excess heat due to work load, temperature-dependent thermal conductivity is of particular interest.

Based on the kinetic theory, by solving the phonon Boltzmann transport equation (BTE), the lattice thermal conductivity (κ) of semiconductors and insulators can be expressed as [7]

$$\kappa_\alpha = \sum_{\vec{q}p} C_V v_\alpha(\vec{q},p)^2 \tau(\vec{q},p) , \quad (1)$$

where C_V is volumetric specific heat capacity, $\vec{v}_\alpha(\vec{q},p)$ is the $\alpha(=x,y,z)$ component of the group velocity of the phonon mode, with wave vector $\vec{q}$ and polarization p, and τ is the relaxation time (lifetime). Usually, κ is affected by temperature due to the temperature-dependent heat capacity and phonon lifetime, while the phonon group velocity is assumed to be temperature independent. (This assumption is generally reasonable unless the material has a considerably large thermal expansion coefficient.) At low temperatures there are few phonons excited. The mean free path (MFP, $l = \vec{v}\tau$) is very large and is limited by the crystal size. Thus κ is only limited by the heat capacity and is proportional to T^3 from the Debye approximation (the Debye T^3 law). The T^3 relationship holds in a wide domain up to a significant fraction of the Debye temperature (Θ_D). As temperature goes up beyond the Debye temperature, the MFP is limited by the phonon-phonon scattering (mainly through the U process). Since the heat capacity saturates and is almost independent of temperature at high temperature (the Dulong-Petit law) [8], the thermal conductivity is governed by MFP and is proportional to $1/T^\alpha$, where $\alpha \approx 1$ for most cases. However, the fast $1/T$ drop of

*hum@ghi.rwth-aachen.de

 ©2017 American Physical Society

thermal conductivity with temperature increasing is harmful for nanoelectronics in terms of efficient heat dissipation. Therefore, pursuing semiconductor materials that possess slow decay of thermal conductivity with temperature is extremely important for the future development of nanoelectronics.

GaN-based devices, which usually work in high power density, have long been studied for their applications in optoelectronics in the visible and ultraviolet spectral ranges, such as photodetectors, LEDs, lasers, and solar cells [9–15]. Notably, the Nobel Prize in Physics 2014 was awarded jointly to Isamu Akasaki, Hiroshi Amano, and Shuji Nakamura "for the invention of efficient blue light-emitting diodes which has enabled bright and energy-saving white light sources," which is implemented mainly based on GaN [16]. Recently, monolayer GaN with a planar honeycomb structure was successfully fabricated in experiments by reconstructing the wurtzite bulk GaN into a 2D graphitic structure [17,18]. So far, research works of monolayer GaN have been conducted focusing on the electrical/optical properties and current-voltage characteristics, promising its potential applications in nano- and optoelectronics, such as light emitting diodes and lasers [18–21]. Considering that all these applications of monolayer GaN are inevitably involved with heat dissipation, systematic investigation of the thermal transport properties of 2D GaN is in demand.

In this paper, based on first-principles calculations, we comprehensively investigate the phonon transport in monolayer GaN, especially the temperature-dependent thermal conductivity. Despite the commonly established $1/T$ relation of thermal conductivity for lots of materials, we find that monolayer GaN exhibits anomalous behavior that the thermal conductivity almost decreases linearly in a wide temperature range above 300 K. Consequently, the thermal conductivity at high temperature is much higher than the expected thermal conductivity that follows the general $\kappa \sim 1/T$ trend, which would be beneficial for the applications of monolayer GaN in nano- and optoelectronics in terms of efficient heat dissipation. We perform detailed analysis on the mechanisms underlying the anomalously temperature-dependent thermal conductivity of monolayer GaN in the framework of BTE and further gain insight from the view of electronic structure. The fundamental understanding of phonon transport in monolayer GaN gained from this study is of great significance for the design and search of materials superior for applications in nano- and optoelectronics in terms of high-performance thermal management.

II. METHODS

All the first-principles calculations are performed based on the density functional theory (DFT) using the projector augmented wave (PAW) method [22] as implemented in the Vienna *ab initio* simulation package (VASP) [23]. The Perdew-Burke-Ernzerhof (PBE) [24] of the generalized gradient approximation (GGA) is chosen as the exchange-correlation functional. The kinetic energy cutoff of wave functions is set as 1000 eV (see Fig. S1 in the Supplemental Material [25]), and a Monkhorst-Pack [26] k mesh of $15 \times 15 \times 1$ is used to sample the Brillouin zone (BZ), with the energy convergence threshold set as 10^{-6} eV. A large vacuum spacing of 20 Å along the *out-of-plane* direction is used to avoid the interactions between the layer and its mirrored image arising from the periodic boundary conditions employed. All geometries are fully optimized until the maximal Hellmann-Feynman force is no larger than 10^{-5} eV/Å. For the calculation of interatomic force constants (IFCs), a $5 \times 5 \times 1$ supercell containing 50 atoms is constructed and the Monkhorst-Pack k mesh of $2 \times 2 \times 1$ is used to sample the BZ (see Fig. S2 in the Supplemental Material [25]). The space group symmetry properties are used to reduce the computational cost and the numerical noise of the forces [27]. The translational and rotational invariance of IFCs are enforced using the Lagrange multiplier method [28,29]. The Born effective charges (Z^*) and dielectric constants (ϵ) are obtained based on the density functional perturbation theory (DFPT), which is added to the dynamical matrix as a correction to take long-range electrostatic interactions into account. The thickness of monolayer GaN is chosen as the largest *van der Waals* diameter of gallium atoms (3.74 Å). The κ is obtained by solving the linearized phonon BTE using an iterative procedure as implemented in the ShengBTE code [29,30], which is equivalent to the solution of relaxation time approximation (RTA) if the iteration stops at the first step. The full solution of BTE provides mode-dependent nonequilibrium populations to calculate phonon-phonon scattering rates. The obtained lifetime can be interpreted based on the concept of relaxon (collective phonon excitations), which is defined as the eigenstates of the scattering matrix and serves as the energy transport carriers [31]. Based on the convergence test of thermal conductivity, we choose the cutoff interactions up to the 5th nearest neighbors (corresponding to the cutoff distance of 6.1 Å) and the Q grid of $101 \times 101 \times 1$ (see Fig. S3 in the Supplemental Material [25]). The effect of finite size on κ is addressed by considering the phonon boundary scattering based on the Matthiessen rule [32].

III. RESULTS

A. Orbitally driven strong polarization and LO-TO splitting

Monolayer GaN possesses a graphenelike planar honeycomb geometry structure, with the two carbon (C) atoms in the primitive cell substituted by gallium (Ga) and nitrogen (N) atoms, respectively. The lattice constant of the optimized structure using GGA-PBE is 3.255 Å, which is in good agreement with previous reports [33]. The space symmetry group is P-$6M2$, lower than that of graphene ($P6/MMM$) due to the broken symmetry. Despite the similar geometry structure of monolayer GaN as graphene and silicene, their charge density difference is different. As revealed in Figs. 1(a) and 1(b), the covalent bond in monolayer GaN is strongly polarized, which is due to the large difference in the electronegativity between Ga and N atoms [34]. To gain insight into how the strongly polarized bond in monolayer GaN originates, we perform analysis based on the orbital projected electronic structure. As shown in Fig. 1(c), the bonding states near the valence band maximum (VBM) is mainly contributed from the N-p orbital, while the contribution from the Ga-p orbital is minor. Thus, the Ga-d mediated sp^2 hybridization Ga-N bond is strongly polarized due to the unbalanced contribution from Ga and N atoms [34]. The strongly polarized covalent bond

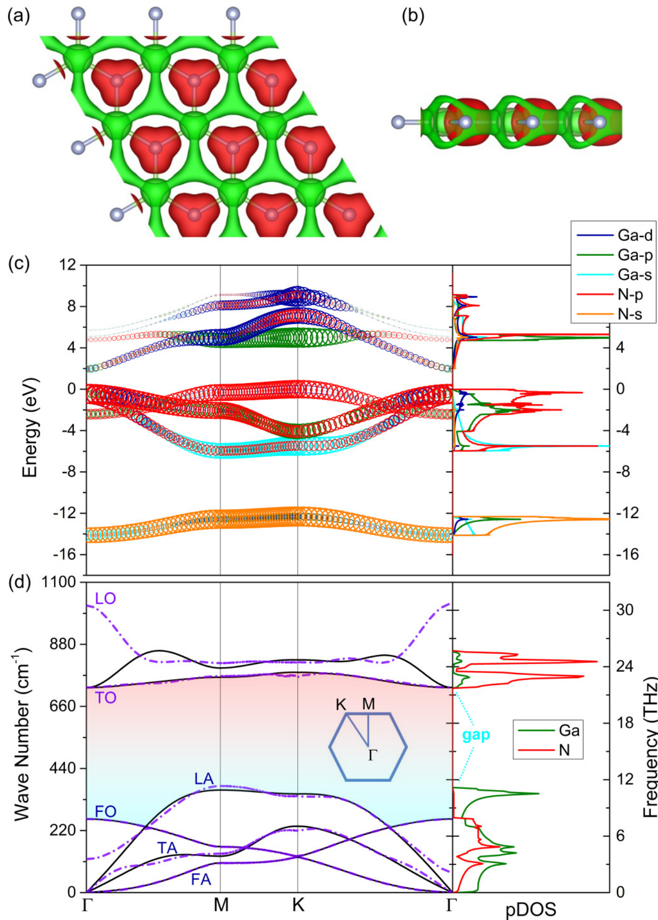

FIG. 1. Electronic and phononic properties of monolayer GaN. (a) Top view and (b) side view of monolayer GaN structure. Isosurface plot at the level of 0.007 $e\text{Å}^{-3}$ is the charge density difference (total density minus the sum of atomic densities; red: positive, green: negative). (c) Orbital projected electronic structure of monolayer GaN. The bonding states near the valence band maximum are mainly contributed by the N-p orbital, which is hybridized with the Ga-p orbital and mediated by the Ga-d orbital. (d) Phonon dispersions and partial density of states (pDOS) of monolayer GaN. The phonon dispersion considering the effect of Born effective charges and dielectric constants is plotted in a violet dash-dot line, showing LO-TO splitting at the center of the BZ (Γ point). (Inset) The high-symmetry k points in BZ.

is also characterized by large Born effective charges (Z^*) and dielectric constants (ϵ), as given in Table I.

Due to the long-range electrostatic Coulomb interactions, macroscopic electric fields arise from the atomic displacements associated with the long wave longitudinal optical (LO) phonons, which leads to the well-known LO–transverse-optical (TO) splitting (the frequency shift between LO and TO at the BZ center) [35]. The LO-TO splitting is clearly seen in the phonon dispersion [Fig. 1(d)], which results in the enhanced phonon group velocity of the LO branch and then affects the phonon transport properties of monolayer GaN, as we will see later.

Note that there exists a huge gap in the phonon dispersion between LO/TO and other phonon branches. The phonon band gap originates from the huge difference in the atomic mass of Ga and N atoms, which is confirmed by the (atom) partial density of states (pDOS) [Fig. 1(d)]. Also note that the phonon dispersion of monolayer GaN shows no imaginary frequency [Fig. 1(d)], which is similar to that reported by Camacho-Mojica and Lopez-Urias [18] while different from that reported by Sahin *et al.* [33]. The difference might lie in the rough convergence criterion for structural optimization (0.05 eV/Å) used in the work by Sahin *et al.* [33], which is more than 3 orders of magnitude rougher than that used in our work (10^{-5} eV/Å). With a rough convergence criterion, the structure might be not fully optimized, which means that the structure is not at the most stable configuration and imaginary frequency would emerge. Moreover, when approaching to the Γ point in BZ, the longitudinal acoustic (LA) and transverse acoustic (TA) phonon branches of monolayer GaN show linear behavior as that in 3D materials, while for flexural acoustic (FA) phonon branch it shows a quadratic behavior (see Fig. S4 in the Supplemental Material [25]), which is universal for 2D materials and is important for obtaining accurate thermal conductivity [36].

TABLE I. Born effective charges (Z^*) of Ga and N atoms and the dielectric constants (ϵ) of monolayer GaN.

Direction	Z^*(Ga)	Z^*(N)	ϵ
xx	3.213065	–3.213065	1.871409
xy	0	0	0
xz	0	0	0
yx	0	0	0
yy	3.212515	–3.212515	1.871393
yz	0	0	0
zx	0	0	0
zy	0	0	0
zz	0.342835	–0.342835	1.148246

B. Anomalously temperature-dependent thermal conductivity

The thermal conductivity of monolayer GaN at room temperature calculated by solving the phonon BTE with the iterative method is 14.9 $\text{W m}^{-1}\text{K}^{-1}$, which is on the similar magnitude as that of silicene [39] (∼20 $\text{W m}^{-1}\text{K}^{-1}$) while significantly lower than that of graphene [47] (∼3000 $\text{W m}^{-1}\text{K}^{-1}$). The thermal conductivity obtained based on RTA is 12.3 $\text{W m}^{-1}\text{K}^{-1}$, which only underestimates the accurate thermal conductivity (obtained by the iterative method) by 17.76%. The underestimation is on the same magnitude as that of silicene (17.5%), while much less than that of graphene (83.4%) [39,48,49]. When the Born effective charges (Z^*) and dielectric constants (ϵ) are neglected, the thermal conductivity obtained using the iterative method is 24.9 $\text{W m}^{-1}\text{K}^{-1}$, which corresponds to an overestimation of 66.71%. The large overestimation results from the removal of long-range electrostatic Coulomb interactions in such polar crystal, which reduces the scattering of phonons and thus enhances the thermal conductivity. The changed scattering of phonons is related to the activation and deactivation of phonon modes due to the change of the phonon frequency. With the long-range interactions and LO-TO splitting, LO phonon modes increase in energy and are not fully active at 300 K, which may cause

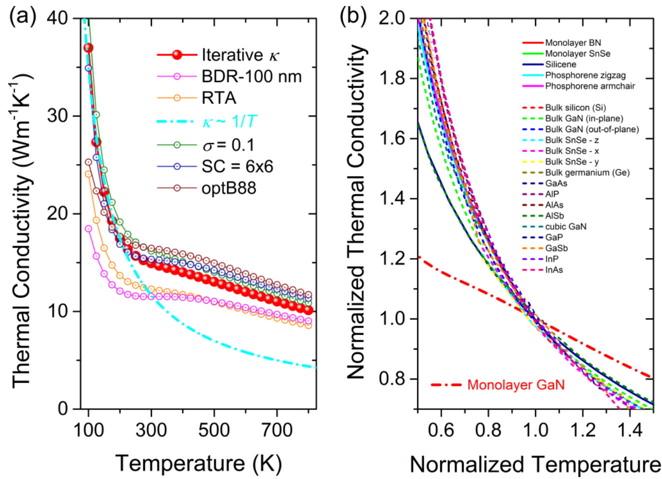

FIG. 2. (a) Temperature (100–800 K) dependent thermal conductivity (absolute value) of monolayer GaN calculated using the iterative method. The results by considering boundary (BDR) scattering with finite length of 100 nm and that calculated with the RTA method are also plotted. Moreover, the results calculated respectively with a smaller broadening parameter for phonon-phonon scattering δ function ($\sigma = 0.1$), or with a larger supercell (6×6), or including the *van der Waals* interactions (optB88 exchange functional) are also plotted, which agree well with each other and confirm the solidity of the anomalous temperature dependence relation. The $\kappa \sim 1/T$ relation is plotted for comparison. (b) Comparison of temperature-dependent thermal conductivity between various materials [3,4,37–46] and monolayer GaN. The temperature is normalized with their respective Debye temperatures. All the thermal conductivities are normalized with the values at their respective Debye temperatures.

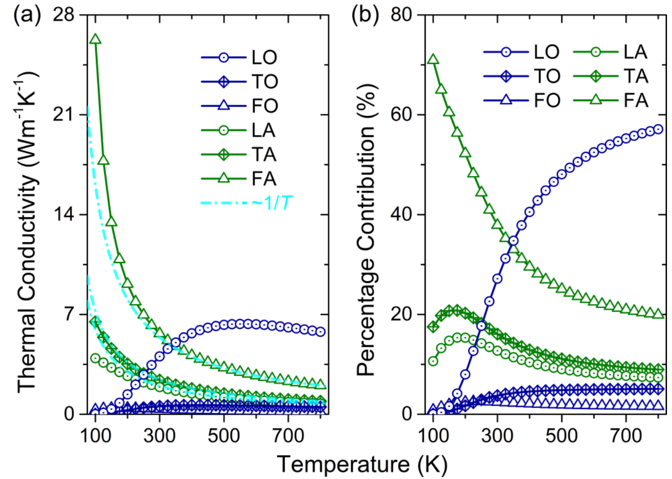

FIG. 3. (a) The absolute and (b) the relative contribution (percentage) to the total thermal conductivity of monolayer GaN from each individual phonon branch as a function of temperature. The $\kappa \sim 1/T$ curve is plotted in dash-dot for indicating the variation trend of three acoustic phonon branches.

different scattering channels and then the reduced thermal conductivity.

The most striking result illustrated in Fig. 2 is that the thermal conductivity of monolayer GaN shows an anomalous linear dependence with temperature above ∼300 K, deviating largely from the well-known $\kappa \sim 1/T$ relationship. The temperature dependence of thermal conductivity of monolayer GaN is totally different from that for common crystalline materials. The temperature-dependent thermal conductivity of lots of crystalline materials in both bulk (3D) and monolayer (2D) forms [Fig. 2(b)] follows the relation of $\kappa \sim 1/T^{\alpha}$ very well, with the value of α ranging from 0.85 to 1.05 [3,4,37–46]. The almost linearly temperature-dependent thermal conductivity of monolayer GaN indicates that the thermal conductivity at high temperatures is higher than the expected value that follows the general trend of $\kappa \sim 1/T$ [Fig. 2(a)], which would be very beneficial for the applications of monolayer GaN in nano- and optoelectronics in terms of efficient heat dissipation. In Fig. 2(a) we also plot the temperature-dependent thermal conductivity by considering the phonon boundary (BDR) scattering due to finite size of 100 nm, which is much longer than the representative MFP of monolayer GaN at 300 K (21.6 nm) (denoted as BDR-100 nm), and the results obtained by RTA. Moreover, we calculate the thermal conductivity of monolayer GaN, respectively, with a smaller broadening parameter for a phonon-phonon scattering δ function ($\sigma = 0.1$), or with a larger supercell (6×6), or including the *van der Waals* interactions (optB88 exchange functional), as plotted in Fig. 2(a). All the results with different parameters show good agreement with each other, which confirms the anomalous temperature dependence of thermal conductivity of monolayer GaN.

To understand the underlying mechanism responsible for the anomalous temperature dependence of thermal conductivity of monolayer GaN, we plot the absolute contribution from each phonon branch [FA, TA, LA, FO, TO and LO as marked in Fig. 1(d)] to the overall thermal conductivity in Fig. 3(a), with the relative percentage contribution plotted in Fig. 3(b). For temperatures lower than 350 K, the FA branch dominates the phonon transport in monolayer GaN, which is similar to that in graphene. Because of the reflectional symmetry of the planar honeycomb structure of monolayer GaN, the phonon scattering processes involving odd numbers of FA phonon modes are largely suppressed, which is the so-called symmetry-based selection rule of phonon-phonon scattering [47]. The suppression of phonon scattering of FA phonon modes results in low scattering rates that are equivalent to large phonon lifetimes, and finally leads to the dominant contribution to the thermal conductivity. Besides, it is clearly shown in Fig. 3(a) that the temperature-dependent contribution from three acoustic phonon branches matches very well with the general ∼$1/T$ trend. Thus the temperature-dependent thermal conductivity would match with the relation of $\kappa \sim 1/T$ if acoustic phonon branches dominate the phonon transport, as is the case for most materials [Fig. 2(b)]. However, the situation for monolayer GaN is quite different. With temperature increasing, the contribution from FA decreases while the contribution from LO increases. When the temperature is around 350 K, there is a crossover in the thermal conductivity contribution between FA and LO branches. Afterwards, the LO overwhelms FA and starts to dominate phonon transport in monolayer GaN. A closer look at Fig. 3(a) reveals that the absolute contribution from LO first increases and then begins to slowly decrease with temperature increasing, which leads to the anomalous

temperature dependence of thermal conductivity of monolayer GaN. The turning point is 550 K, which is also the turning point where the percentage contribution from LO begins to be larger than 50%, as shown in Fig. 3(b). Note that although the absolute contribution from LO begins to slowly decrease when temperature rises above 550 K [Fig. 3(a)], its percentage contribution keeps increasing [Fig. 3(b)] due to decrease of the total thermal conductivity. From above analysis, we find that the anomalous linear temperature dependence of thermal conductivity of monolayer GaN is a direct consequence of the competition in the thermal conductivity contribution between acoustic phonon branches (e.g., FA) and optical phonon branches (e.g., LO).

Here we would like to note that the different branches and their contribution to the thermal conductivity are simply determined based on the increasing order of energy. The procedure is effective for three reasons: (1) The thermal conductivity is dominated by LO, and then mostly contributed by FA. LO and FA together contribute ∼80% to the total thermal conductivity [Fig. 3(b)]. Based on the 3D phonon dispersion in the whole BZ (see Fig. S5 in Supplemental Material [25]), the LO and FA can be clearly identified because of no crossover with other branches. (2) The crossover happens only for FO, LA, and TA. Considering the small contribution to the thermal conductivity from these three phonon branches, the error in the values caused by the crossover can be neglected, which will not affect the major conclusion of our analysis. (3) In the reciprocal space, different branches form different surfaces and they cross over with each other and transfer to each other smoothly. Thus, it is impossible to rigorously determine which phonon branch one point in the reciprocal space (polarization and **q** vector) belongs to if crossover happens. For example, from Γ-M-K-Γ in monolayer GaN, the FO transfers smoothly to FA and FA also smoothly transfers to FO. The similar smooth transfer is also observed in other materials such as phosphorene [4]. In short, currently it is difficult to rigorously determine the phonon branch in the whole reciprocal space when crossover happens, and we look forward to future work addressing this problem. As for the specific case of monolayer GaN, the method simply based on the increasing order of energy is already effective to get insight into the contribution to thermal conductivity from different phonon branches, such as FA and LO.

Based on the above discussions, we know that to realize the slow decay of thermal conductivity with temperature increasing, such as the linear temperature dependence of thermal conductivity of monolayer GaN presented herein, the following two conditions must be fulfilled:

(1) The contribution to thermal conductivity from optical phonon branch(es) should increase with temperature increasing.

(2) The optical phonon branch(es) should dominate phonon transport at high temperature.

Note that only if the two conditions are both fulfilled can the temperature dependence of thermal conductivity be so anomalous, i.e., thermal conductivity largely deviates from the traditional $1/T$ law. In the following, we discuss these two conditions in sequence and explain why monolayer GaN is so special to hold true for both conditions.

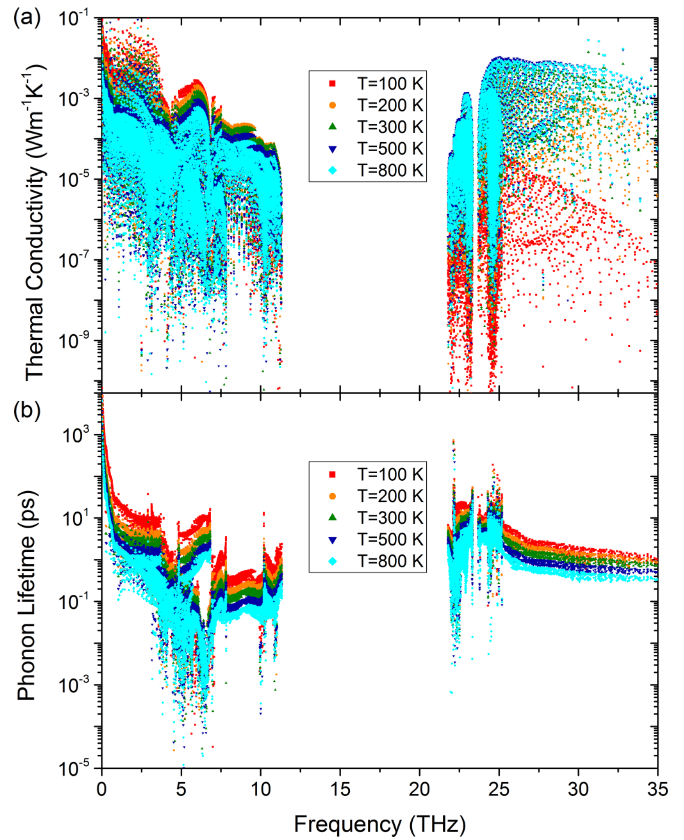

FIG. 4. Comparison of the mode-level (a) contribution to thermal conductivity and (b) phonon lifetime among several representative temperatures.

C. Mode-level analysis

To get insight into the phonon transport in monolayer GaN, first we extract the mode-level contribution to the thermal conductivity and the corresponding phonon lifetime at several representative temperatures, as shown in Fig. 4. The contribution from acoustic phonon modes decreases with temperature increasing, while the variation trend is opposite for optical phonon modes. The mode-level information is consistent with the results presented in Fig. 3. It is clearly shown in Fig. 4(b) that for all phonon modes the lifetime always decreases with temperature increasing, which is consistent with the common knowledge as illustrated in Fig. 2(b). Since the phonon group velocity is assumed to be temperature independent (the validity will be proved below), the root reason for the increased contribution from optical phonon modes must lie in the effect of heat capacity, according to Eq. (1).

D. Heat capacity and phonon group velocity

We then plot the heat capacity of monolayer GaN in Fig. 5(a). Although overall the heat capacity increases with temperature, there is some difference in the frequency-dependent heat capacity between low-frequency acoustic phonon modes and high-frequency optical phonon modes. To make the difference clear, we study the frequency-resolved heat capacity based on the Einstein model, as plotted in

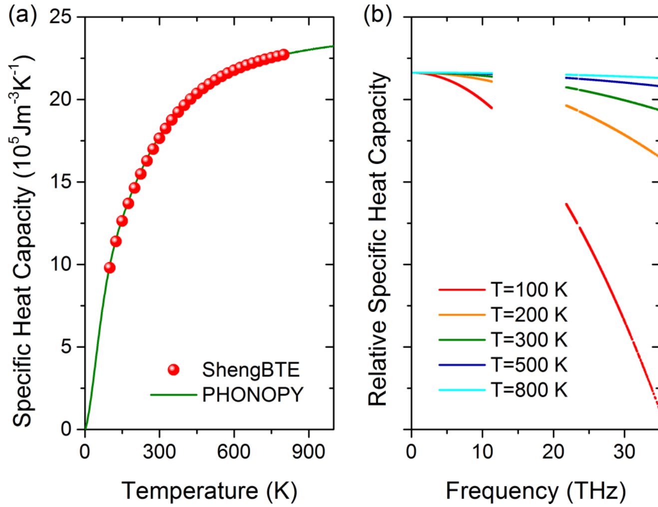

FIG. 5. (a) Heat capacity of monolayer GaN as a function of temperature calculated from the two different procedures. (b) Relative heat capacity as a function of frequency at several representative temperatures based on the Einstein model.

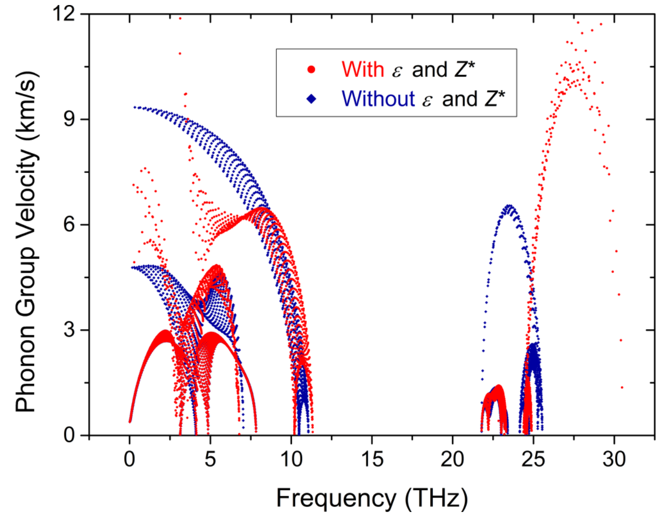

FIG. 6. Comparison of the mode-level phonon group velocity of monolayer GaN with and without the Born effective charges (Z^*) and dielectric constants (ϵ) considered.

Fig. 5(b). It shows that the heat capacity increases much faster for high-frequency optical phonon modes than low-frequency acoustic phonon modes, especially at low temperature. The difference can be intuitively understood from the view of thermal excitation. The lower the frequency the lower the required temperature for thermal activation. Thus, the low-frequency acoustic phonon modes can be much easier thermally activated and already saturate at a lower temperature than the concerned temperatures, whereas the high-frequency optical phonon modes above the phonon band gap, as shown in Fig. 1(d), just begin to be thermally activated around the concerned temperatures, contributing mostly to the increase of the heat capacity. Considering the competition between heat capacity and phonon lifetime, the variation of temperature-dependent contribution to the overall phonon transport from acoustic phonon modes is dominated by the phonon lifetime and decreases with temperature increasing, whereas for optical phonon modes, the variation is dominated by the heat capacity at low temperature due to its fast increase and the contribution increases quickly with temperature increasing. At high temperature, because the heat capacity increases slowly with temperature, the variation of contribution from optical phonon modes becomes visibly affected by phonon lifetime and decreases with temperature increasing (similar to that for acoustic phonon modes). Therefore, as discussed above, the contribution to total thermal conductivity from the LO branch first increases and then begins to slightly decrease with temperature increasing further, with the turning point being around 550 K [Fig. 3(a)].

From the frequency-resolved heat capacity we know that the high-frequency optical phonon modes possess relatively low heat capacity compared to low-frequency acoustic phonon modes. However, at high temperature, the high-frequency optical phonon modes (such as LO) dominate phonon transport in monolayer GaN, and the reason lies in the large group velocity and large lifetime. As discussed above, there exists giant LO-TO splitting in the phonon dispersion of monolayer GaN due to the strongly polarized covalent bond (Fig. 1). The LO-TO splitting results in enhanced phonon group velocity of the LO branch, as shown in Fig. 6, which is the partial reason for LO dominating the thermal conductivity of monolayer GaN. Note that the dominating role and such considerably large group velocity of optical phonon modes is rarely reported in literature. During the review process, we noticed a very recently published paper by Lindsay and Kuang [50]. They report an unusual crossover from acoustic-dominated to optic-dominated thermal transport behavior by increasing mass of the functional group, and connect the crossover to changes in phonon dispersions which suppress velocity of acoustic phonon modes but give unusually high velocity of optical phonon modes [50,51]. In the following, we further analyze the LO dominating thermal conductivity from another aspect of phonon lifetime, and fundamental insight can be gained from the scattering processes (channels).

E. Scattering processes and channels

From the mode-level phonon lifetime as shown in Fig. 4(b), it is found that the lifetime of optical phonon modes (such as LO) is on the same order of magnitude as that of acoustic phonon modes and some of them are even larger. To understand this, we plot the mode-level scattering phase space and scattering rate in Figs. 7(a) and 7(b), respectively. The scattering phase spaces are plotted for the absorption and emission process, respectively. For the scattering rate, we also plot that for the N/U process. The small scattering rate of optical phonon modes as shown in Fig. 7(b) is consistent with their large phonon lifetime, which is another reason for the LO-dominating phonon transport in monolayer GaN in addition to the large group velocity. It is worth noting in Fig. 7(b) that the N process only has a small proportion of the total scattering rate, due to which the thermal conductivity obtained by RTA is only underestimated by 17.76% compared to the accurate iterative method, as discussed above.

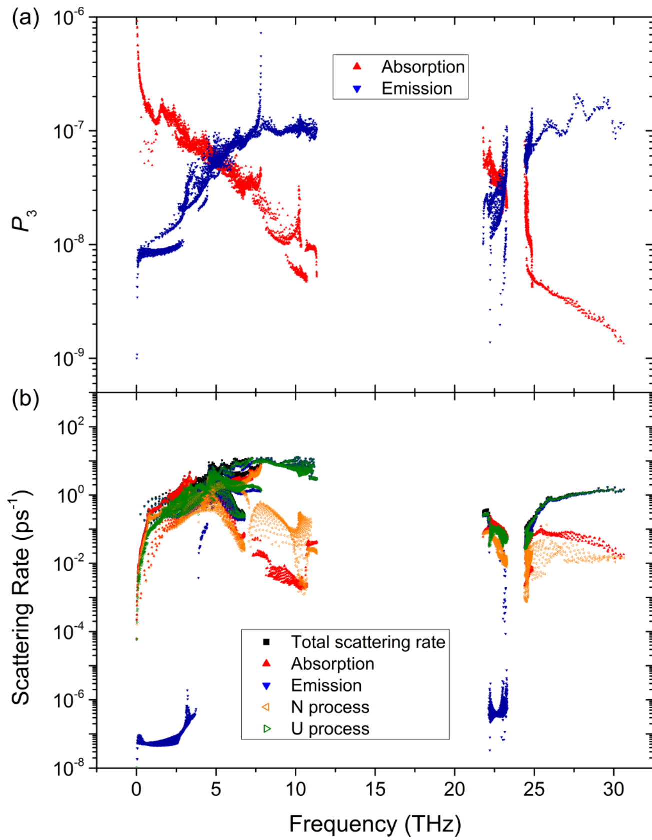

FIG. 7. (a) The mode-level scattering phase space of absorption and emission processes. (b) The mode-level scattering rate decomposed into absorption/emission or N/U process.

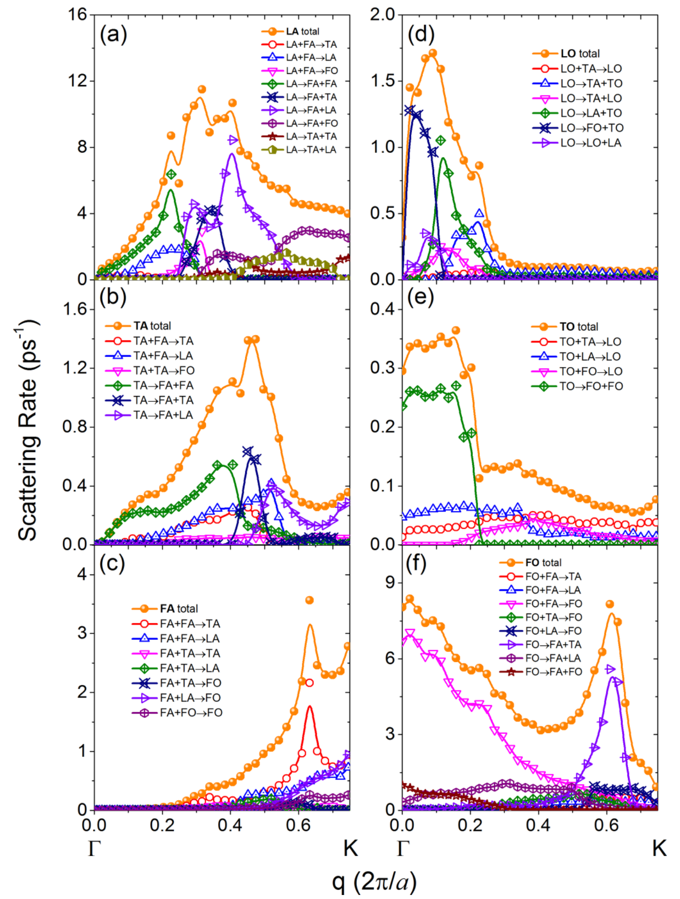

FIG. 8. Scattering channels of phonon modes along the Γ-K direction for (a) LA, (b) TA, (c) FA, (d) LO, (e) TO, and (f) FO phonon branches of monolayer GaN.

The phonon scattering channels ruled by the conservation of energy and momentum quantify the specific scattering processes among different phonon branches, which can provide fundamental insight into the phonon scattering process [38,39,52]. Since the phonon branches are commonly degenerated or cross with each other in most segments of the paths passing through the high-symmetry k points in the BZ [Fig. 1(d)], we only present the detailed scattering process of each phonon branch along the Γ-K direction (Fig. 8), where the phonon modes can be easily separated into different branches, and the crossover problem is fixed manually. The scattering rates for emission processes are multiplied by 1/2 to avoid counting twice for the same process. For the FA phonon branch, the main scattering channel is FA+FA → TA/LA, which is governed by the so-called symmetry-based selection rule of phonon-phonon scattering [47]. However, there exist also narrow scattering channels involving odd numbers of FA, such as FA+LA → FO, which might be due to the slightly broken symmetry by the different diameters and mass of atoms Ga and N despite the planar structure of monolayer GaN. The extra scattering channels lead to the relatively lower contribution to thermal conductivity from FA (37.9%) compared with that in graphene (85%) [47]. For the LO phonon branch, the main scattering channel is LO → FO+TO. That is to say, LO is mainly scattered into optical phonon modes in the emission process, which is consistent with the large phase space and the scattering rate of emission process as shown in Fig. 7. This also means that LO is weakly coupled with acoustic phonon modes because the energy conservation is hard to fulfill for the scattering process due to the huge gap in the phonon dispersion [Fig. 1(d)]. The phonon lifetime of LO is relatively large due to the weak scattering. Hence, the LO phonon branch dominates thermal conductivity of monolayer GaN, which primarily lies in the large phonon group velocity and lifetime. Together with the increased contribution to thermal conductivity with temperature increasing as discussed above, LO competes with the acoustic phonon branches (e.g., FA), resulting in the slow decay of temperature-dependent thermal conductivity in monolayer GaN.

F. Quasiharmonic approximation

Before closing, we would like to address the assumption we made at the beginning: the same atomic structure configuration optimized at 0 K is used for all temperatures when calculating the temperature-dependent thermal conductivity, i.e., the phonon group velocity is assumed to be temperature independent, and the effect of temperature on the thermal conductivity is only considered through heat capacity and phonon lifetime. It is well known that the phonon group velocity depends on the bonding strength, which is primarily determined by the bonding length, relative atomic position, and lattice constant [53]. With the quasiharmonic approximation

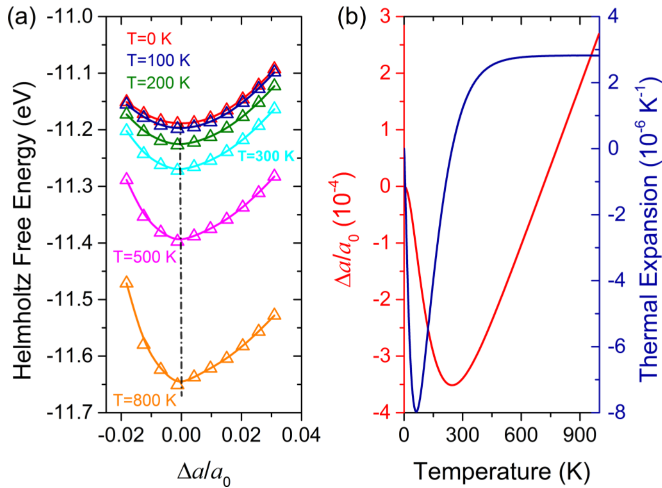

FIG. 9. Results from the quasiharmonic approximation (QHA). (a) The free energy of monolayer GaN as a function of strain (volume change) at several representative temperatures. The dash-dot line guides the equilibrium position. (b) The relative change of the lattice constant (volume) with respect to that at 0 K and the thermal expansion coefficient as a function of temperature.

(QHA), the temperature-dependent properties can be obtained by considering the anharmonic effect, such as Helmholtz free energy, crystal volume, and thermal expansion coefficient [27]. A part of the temperature effect can be included in the total energy of the electronic structure through the phonon (Helmholtz) free energy at constant volume. Gibbs free energy is defined at a constant pressure by the transformation of $G(T,p) = \min_V[U(V) + F_{\text{phonon}}(T;V) + pV]$, where the $\min_V$ function means to find unique minimum value by changing the volume. Since volume dependencies of energies in electronic and phonon structures are different, the volume giving the minimum value of the energy function in the square brackets shifts from the value calculated only from electronic structure even at 0 K. By increasing the temperature, the volume dependence of phonon free energy changes and then the equilibrium volume at temperatures changes. This is considered as thermal expansion under the QHA.

Figure 9 shows that the variation of the lattice constant is very small (∼0.03%) over the entire temperature range (0–1000 K) considered. Such a small positive/negative thermal expansion almost has no effect on the phonon group velocity and only changes the thermal conductivity by ∼5.8% as we estimated. Therefore, the assumption of the temperature-independent group velocity is reliable, and the anomalous temperature dependence of thermal conductivity still holds even if the thermal expansion due to the temperature (anharmonic) effect is fully considered. In fact, considering thermal expansion of the honeycomb lattice will slightly increase the thermal conductivity of monolayer GaN at high temperature, which makes the temperature-dependent thermal conductivity deviate even further away from the $\kappa \sim 1/T$ law. It is also interesting to note that monolayer GaN possesses a negative thermal expansion coefficient at temperatures below ∼246 K [Fig. 9(b)].

IV. DISCUSSIONS AND CONCLUSIONS

Based on the study of phonon transport in the emerged monolayer GaN, we report the anomalous temperature dependence of thermal conductivity, which deviates largely from the traditional $\kappa \sim 1/T$ law. Two required conditions are proposed for the realization of the anomalous behavior: (1) The contribution to thermal conductivity from optical phonon branch(es) should increase with temperature increasing. (2) The optical phonon branch(es) should dominate phonon transport at high temperature. Detailed analysis is performed to explain why monolayer GaN is so special to hold for both conditions. The first condition lies in the competing effect of heat capacity and phonon lifetime with temperature increasing. For high-frequency optical phonon modes above the phonon band gap, the variance trend is driven by the heat capacity, which keeps increasing with temperature. The required higher temperature for the thermal activation of high-frequency optical phonon modes is responsible for the observed anomalous behavior. The second condition is traced back to the enhanced phonon group velocity and large phonon lifetime. We reveal that the Ga-N bond in monolayer GaN is strongly polarized [Figs. 1(a) and 1(b)], which leads to the LO-TO splitting due to the macroscopic electric fields driven by the long-range electrostatic Coulomb interactions. Enhanced phonon group velocity of the LO branch is caused by the LO-TO splitting (Fig. 6), which is the partial reason for LO dominating the thermal conductivity of monolayer GaN. Deep analysis from the view of electronic structure reveals that the strongly polarized covalent bond is attributed to the special Ga-d mediated sp^2 hybridization Ga-N bond. The bonding states near the VBM are mainly contributed from the N-p orbital, while the contribution from the Ga-p orbital is minor, leading to an unbalanced contribution to the bonding from Ga and N atoms. Thus, the electronic origin of the enhanced phonon group velocity of LO is fundamentally traced back to the special Ga-d mediated sp^2 hybridization of the Ga-N bond. Besides, from the analysis based on the scattering processes and scattering channels, the large phonon lifetime of LO is found to originate from the huge phonon band gap in the phonon dispersion, which lies in the large difference in the atomic mass of Ga and N atoms. Therefore, the LO phonon branch dominates the thermal conductivity of monolayer GaN. Together with the increased contribution to thermal conductivity with temperature increasing, as discussed above for the first condition, LO competes with acoustic phonon branches (e.g., FA), resulting in the anomalous temperature dependence of thermal conductivity in monolayer GaN.

The 2D GaN studied in this work is in the freestanding form, whose stability is always a challenge for practical applications. It might be more stable low-buckled structure when supported on some substrate in practical synthesis routes [17]. In the case of substrate support, the thermal transport properties of 2D GaN would change a lot due to effect of the substrate, which would be different for different substrates. Thus the applicability of the anomalous temperature dependence of thermal conductivity would be critical and depends on the specific substrate. Further studies are anticipated to address these questions on the substrates, which are very interesting and deserve lots of study.

Finally, we would also like to mention that, considering the underlying mechanism for the anomalously temperature-dependent thermal conductivity of monolayer GaN as analyzed above, and the similar phonon band structures as reported by previous studies [33,54], we predict that similar phenomena may also exist in a series of materials with a large difference in atom mass (large phonon band gap) and electronegativity (strongly polarized covalent bond), just name a few: PL-GeC, LB-SiGe, LB-SnSi, PL-SnC, LB-GaP, PL-SiC, PL-AlN, PL-InN, LB-InP, LB-InAs, PL-BP, PL-BAs, LB-AlSb, LB-BSb, PL-ZnO, PL-ZnS (LB: low-buckled; PL: planar). Note that for the low-buckled materials, the FA phonon branch will contribute much less due to the breaking of the selection rule for phonon-phonon scattering. Due to the relatively smaller contribution from the acoustic phonon branches, the anomalously temperature-dependent behavior could be more remarkable. Certainly, one should also consider the other two acoustic phonon branches (LA and TA). The decreased contribution from FA could go to these two other acoustic phonon branches and optical phonon branches as well, which deserves detailed research case by case.

In summary, we have performed a comprehensive study on the phonon transport properties of monolayer GaN, with a focus on the temperature-dependent thermal conductivity. Despite the commonly established $1/T^{\alpha}$ ($\alpha \approx 1$) relationship for the thermal conductivity of a tremendous amount of materials based on the kinetic theory and BTE, monolayer GaN is found to possess anomalously linear temperature-dependent thermal conductivity. The large deviation from the $1/T$ law stems from the LO phonon branch, whose contribution to total thermal conductivity increases with the temperature increase and eventually dominates the phonon transport by overwhelming the acoustic phonon branches (mainly FA). We provide explanations to the increase in the contribution from LO by analyzing the competing mechanism of frequency-resolved heat capacity and phonon lifetime. Furthermore, the underlying mechanism for LO dominating thermal conductivity is traced back to the enhanced phonon group velocity and large phonon lifetime. The enhanced phonon group velocity is due to the giant LO-TO splitting resulting from the orbitally driven strongly polarized covalent bond in monolayer GaN. From the analysis based on the scattering processes and scattering channels, the large phonon lifetime of LO is found due to the huge phonon band gap in the phonon dispersion, which lies in the large difference in the atomic mass of Ga and N atoms. Finally, the reliability of the anomalous temperature dependence of the thermal conductivity is confirmed by performing calculations based on the quasiharmonic approximation that fully addresses the thermal expansion due to temperature (anharmonic) effect. In addition, two required conditions for other materials to exhibit similar anomalous temperature dependence of thermal conductivity as monolayer GaN are also proposed, which would shed light on the design and search of materials superior for applications in nano- and optoelectronics in terms of efficient heat dissipation. Our study offers a fundamental understanding of the interesting phonon transport properties of monolayer GaN, which has great impact on its promising applications in nanoelectronics.

ACKNOWLEDGMENTS

G.Q. would like to thank Mr. Sheng-Ying Yue and Ms. Biyao Wu (RWTH Aachen University) for their fruitful discussions on QHA. This work is supported by the Deutsche Forschungsgemeinschaft (DFG) (Project No. HU 2269/2-1). The authors acknowledge the computing time granted by the John von Neumann Institute for Computing (NIC), the supercomputer JURECA at Jülich Supercomputing Centre (JSC) (Project ID No. JHPC38), and Jülich Aachen Research Alliance-High Performance Computing (JARA-HPC) from RWTH Aachen University under Projects No. jara0160 and No. rwth0223.

[1] H. O. H. Churchill and P. Jarillo-Herrero, Nat. Nanotechnol. **9**, 330 (2014).

[2] G. Qin, Q.-B. Yan, Z. Qin, S.-Y. Yue, H.-J. Cui, Q.-R. Zheng, and G. Su, Sci. Rep. **4**, 6946 (2014).

[3] G. Qin, Q.-B. Yan, Z. Qin, S.-Y. Yue, M. Hu, and G. Su, Phys. Chem. Chem. Phys. **17**, 4854 (2015).

[4] G. Qin, X. Zhang, S.-Y. Yue, Z. Qin, H. Wang, Y. Han, and M. Hu, Phys. Rev. B **94**, 165445 (2016).

[5] F. Schwierz, J. Pezoldt, and R. Granzner, Nanoscale **7**, 8261 (2015).

[6] N. Han, T. V. Cuong, M. Han, B. D. Ryu, S. Chandramohan, J. B. Park, J. H. Kang, Y.-J. Park, K. B. Ko, H. Y. Kim, H. K. Kim, J. H. Ryu, Y. S. Katharria, C.-J. Choi, and C.-H. Hong, Nat. Commun. **4**, 1452 (2013).

[7] D. A. Broido, A. Ward, and N. Mingo, Phys. Rev. B **72**, 014308 (2005).

[8] L. D. Landau and E. M. Lifshitz, *Statistical Physics Part 1, Course in Theoretical Physics 5,* 3rd ed. (Pergamon Press, New York, 1980), pp. 193–196.

[9] G. Y. Xu, A. Salvador, W. Kim, Z. Fan, C. Lu, H. Tang, H. Morkoç, G. Smith, M. Estes, B. Goldenberg, W. Yang, and S. Krishnankutty, Appl. Phys. Lett. **71**, 2154 (1997).

[10] Y. Taniyasu, M. Kasu, and T. Makimoto, Nature (London) **441**, 325 (2006).

[11] H. Y. Ryu, K. H. Ha, J. K. Son, S. N. Lee, H. S. Paek, T. Jang, Y. J. Sung, K. S. Kim, H. K. Kim, Y. Park, and O. H. Nam, Appl. Phys. Lett. **93**, 011105 (2008).

[12] S. Staadczyk, T. Czyszanowski, A. Kafar, R. Czernecki, G. Targowski, M. Leszczyadski, T. Suski, R. Kucharski, and P. Perlin, Appl. Phys. Lett. **102**, 151102 (2013).

[13] C. J. Neufeld, N. G. Toledo, S. C. Cruz, M. Iza, S. P. DenBaars, and U. K. Mishra, Appl. Phys. Lett. **93**, 143502 (2008).

[14] Z. Qin, Z. Xiong, G. Qin, and Q. Wan, J. Appl. Phys. **114**, 194307 (2013).

[15] Z. Qin, Z. Xiong, G. Qin, and L. Chen, J. Appl. Phys. **116**, 224503 (2014).

[16] L. Martiradonna, Nat. Mater. **14**, 362 (2015).

[17] Z. Y. Al Balushi, K. Wang, R. K. Ghosh, R. A. Vila, S. M. Eichfeld, J. D. Caldwell, X. Qin, Y.-C. Lin, P. A. DeSario, G. Stone, S. Subramanian, D. F. Paul, R. M. Wallace, S. Datta, J. M. Redwing, and J. A. Robinson, Nat. Mater. **15**, 1166 (2016).

[18] T. H. Seo, A. H. Park, S. Park, Y. H. Kim, G. H. Lee, M. J. Kim, M. S. Jeong, Y. H. Lee, Y.-B. Hahn, and E.-K. Suh, Sci. Rep. **5**, 7747 (2015).

[19] D. C. Camacho-Mojica and F. López-Urías, Sci. Rep. **5**, 17902 (2015).

[20] A. V. Kolobov, P. Fons, J. Tominaga, B. Hyot, and B. Andrar, Nano Lett. **16**, 4849 (2016).

[21] T. Tao, T. Zhi, B. Liu, M. Li, Z. Zhuang, J. Dai, Y. Li, F. Jiang, W. Luo, Z. Xie, D. Chen, P. Chen, Z. Li, Z. Zou, R. Zhang, and Y. Zheng, Sci. Rep. **6**, 20218 (2016).

[22] G. Kresse and D. Joubert, Phys. Rev. B **59**, 1758 (1999).

[23] G. Kresse and J. Furthmüller, Phys. Rev. B **54**, 11169 (1996).

[24] J. P. Perdew, K. Burke, and M. Ernzerhof, Phys. Rev. Lett. **77**, 3865 (1996).

[25] See Supplemental Material at http://link.aps.org/supplemental/10.1103/PhysRevB.95.195416 for the convergence test of computational parameters and detailed information on phonon dispersion.

[26] H. J. Monkhorst and J. D. Pack, Phys. Rev. B **13**, 5188 (1976).

[27] A. Togo, F. Oba, and I. Tanaka, Phys. Rev. B **78**, 134106 (2008).

[28] K. Esfarjani and H. T. Stokes, Phys. Rev. B **77**, 144112 (2008).

[29] W. Li, L. Lindsay, D. A. Broido, D. A. Stewart, and N. Mingo, Phys. Rev. B **86**, 174307 (2012).

[30] W. Li, J. Carrete, N. A. Katcho, and N. Mingo, Comput. Phys. Commun. **185**, 1747 (2014).

[31] A. Cepellotti and N. Marzari, Phys. Rev. X **6**, 041013 (2016).

[32] D. L. Nika, E. P. Pokatilov, A. S. Askerov, and A. A. Balandin, Phys. Rev. B **79**, 155413 (2009).

[33] H. Şahin, S. Cahangirov, M. Topsakal, E. Bekaroglu, E. Akturk, R. T. Senger, and S. Ciraci, Phys. Rev. B **80**, 155453 (2009).

[34] Z. Qin, G. Qin, X. Zuo, Z. Xiong, and M. Hu, Nanoscale **9**, 4295 (2017).

[35] X. Gonze and C. Lee, Phys. Rev. B **55**, 10355 (1997).

[36] J. Carrete, W. Li, L. Lindsay, D. A. Broido, L. J. Gallego, and N. Mingo, Mater. Res. Lett. **0**, 1 (2016).

[37] J.-Y. Yang, G. Qin, and M. Hu, Appl. Phys. Lett. **109**, 242103 (2016).

[38] G. Qin, Z. Qin, W.-Z. Fang, L.-C. Zhang, S.-Y. Yue, Q.-B. Yan, M. Hu, and G. Su, Nanoscale **8**, 11306 (2016).

[39] H. Xie, T. Ouyang, E. Germaneau, G. Qin, M. Hu, and H. Bao, Phys. Rev. B **93**, 075404 (2016).

[40] L. Lindsay and D. A. Broido, Phys. Rev. B **84**, 155421 (2011).

[41] A. Jain and A. J. McGaughey, Comput. Mater. Sci. **110**, 115 (2015).

[42] L. Lindsay, D. A. Broido, and T. L. Reinecke, Phys. Rev. Lett. **109**, 095901 (2012).

[43] C. W. Li, J. Hong, A. F. May, D. Bansal, S. Chi, T. Hong, G. Ehlers, and O. Delaire, Nat. Phys. **11**, 1063 (2015).

[44] J. Carrete, N. Mingo, and S. Curtarolo, Appl. Phys. Lett. **105**, 101907 (2014).

[45] L.-C. Zhang, G. Qin, W.-Z. Fang, H.-J. Cui, Q.-R. Zheng, Q.-B. Yan, and G. Su, Sci. Rep. **6**, 19830 (2016).

[46] L. Lindsay, D. A. Broido, and T. L. Reinecke, Phys. Rev. B **87**, 165201 (2013).

[47] L. Lindsay, D. A. Broido, and N. Mingo, Phys. Rev. B **82**, 115427 (2010).

[48] Y. Wang, A. K. Vallabhaneni, B. Qiu, and X. Ruan, Nanoscale Microscale Thermophys. Eng. **18**, 155 (2014).

[49] X. Gu and R. Yang, J. Appl. Phys. **117**, 025102 (2015).

[50] L. Lindsay and Y. Kuang, Phys. Rev. B **95**, 121404 (2017).

[51] S. Mukhopadhyay, L. Lindsay, and D. J. Singh, Sci. Rep. **6**, 37076 (2016).

[52] H. Liu, G. Qin, Y. Lin, and M. Hu, Nano Lett. **16**, 3831 (2016).

[53] S.-Y. Yue, G. Qin, X. Zhang, X. Sheng, G. Su, and M. Hu, Phys. Rev. B **95**, 085207 (2017).

[54] H. Wang, G. Qin, G. Li, Q. Wang, and M. Hu Phys. Chem. Chem. Phys. (2017), doi: 10.1039/C7CP00460E.